Electronic Supplementary Material (ESI) for Physical Chemistry Chemical Physics.

Supplementary Information

Strain effects of Co, N co-decorated graphyne catalysts on the overall water splitting electrocatalysis

Xiaoping Gao[#a], Yanan Zhou [#b], Yujia Tan[a], Shiqiang Liu[a], Zhiwen Cheng[a], Zhemin Shen*[a,c]

a.School of Environmental Science and Engineering, Shanghai Jiao Tong University, Shanghai,200240, China

b.School of Chemical Engineering, Sichuan University, Chengdu 610065, China

c.Shanghai Institute of Pollution Control and Ecological Security, Shanghai 200092, China

Calculation method of HER and OER activity

The intermediate states in HER (H*) and OER (HO*, O* and HOO*) reactions were tested several different initial configurations on the strain-optimized Co@N_1-GY electrocatalysts. The calculated results are based on the most stable structures. The adsorption energies (ΔE_{ads}) are obtained through the following equation (1):

$$\Delta E_{ads} = E_{substrate + adsorbent} - E_{substrate} - E_{adsorbent} \qquad (1)$$

where the $E_{adsorbent}$, $E_{substrate}$, and $E_{substrate + adsorbent}$ are the total energies of the adsorbent, the substrate, and the substrate-adsorbent composites, respectively. The more negative ΔE_{ads} values represent the stronger binding between catalyst and intermediate as well as the better thermodynamic stability.

For HER, the H_2 generation from water splitting involves two steps: a) the atomic H adsorption on the catalysts; b) the formation and release of H_2 molecular [1]. When

---

*Corresponding author.
E-mail address: zmshen@sjtu.edu.cn.
[#] These authors contributed equally.

one H is adsorbed on the catalyst, the calculated intermediate state energy determines the HER reaction barrier (overpotential for the electron). Thus, we can assess the HER performance through ΔG_{H*}:

$$H^+ + e^- + * \xrightarrow{\Delta G_{H^*}} H^* \tag{2}$$

where H* and * represent the adsorbed intermediate and the active site, respectively. Under the standard conditions (pH=0, U=0, and 298.15 K), the chemical potential of $H^+ + e^-$ ($\mu_{(H+ + e-)}$) is equivalent to that of 1/2 H_2 (1/2 μ_{H2}). Namely, $\mu_{(H+ + e-)} = 1/2\ \mu_{H2}$ is obtained based on the calculation hydrogen electrode model [2]. Thus, the ΔG_{H*} is calculated by:

$$\Delta G_{H*} = \Delta E_{H*} + \Delta E_{ZPE} - T\Delta S_{H*} \tag{3}$$

where ΔE_{H*} means the hydrogen adsorption energy obtained from equation (1). ΔE_{ZPE} means the zero-point energy difference between gas-phase H_2 and the adsorbed H obtained by the equation $\Delta E_{ZPE} = E_{ZPE}^{H*} - E_{ZPE}^{*} - \frac{1}{2}E_{ZPE}^{H2}$, where E_{ZPE}^{*}, E_{ZPE}^{H*}, and E_{ZPE}^{H2} denote the zero-point energies of pure substrate, an adsorbed hydrogen on the substrate, and gas phase H_2, respectively. T means the temperature at 298K and ΔS_{H*} represents the entropy difference between the gas phase and the adsorbed state. Due to the small calculated vibrational entropy of adsorbed state H*, the adsorption entropy of 1/2 H_2 is $\Delta S_H \approx -0.5 S_{H2}^{0}$, where S_{H2}^{0} denotes the entropy of gas phase H_2 and is about 130 $J\cdot mol^{-1}\cdot K^{-1}$at the standard conditions [3]. Interestingly, it is found that the entropy and the ZPE of the adsorbed states on different catalysts show close values (Table S1 and S2). According to Nørskov's assumption [1], the overpotential of HER (η^{HER}) can be written as $|\Delta G_{H*}|/e$. The ideal ΔG_{H*} value for HER is zero. Too strong or too weak binding energy of intermediate state can lead to bad HER performance.

For OER, there are four elementary steps at pH=0 as follows:

$$H_2O(l) + * \xrightarrow{\Delta G_1} HO^* + H^+ + e^- \tag{4}$$

$$HO^* \xrightarrow{\Delta G_2} O^* + H^+ + e^- \tag{5}$$

$$O^* + H_2O(l) \xrightarrow{\Delta G_3} HOO^* + H^+ + e^- \tag{6}$$

$$HOO^* \xrightarrow{\Delta G_4} * + O_2(g) + H^+ + e^- \quad (7)$$

where (g) and (l) are the gas and liquid phases, respectively. HO*, O*, and HOO* are the adsorbed intermediates in OER. The change in Gibbs free energy (ΔG) for every step can be described as:

$$\Delta G = \Delta E + \Delta E_{ZPE} - T\Delta S + \Delta G_U + \Delta G_{pH} \quad (8)$$

where ΔE, ΔS, and ΔE_{ZPE} are the energy difference of adsorption, entropy, and zero-point energy, respectively. The ΔE is calculated from DFT, and the ΔE_{ZPE} as well as TΔS are obtained by DFT and the standard thermodynamic date. $\Delta G_U = -eU$, where U (U=0) and *e* are the potential at the standard hydrogen electrode and the charge transfer, respectively. ΔG_{pH}, which equals $-k_B T\ln 10 * pH$, is the Gibbs free energy corrected by H^+ concentration, and pH=0 is employed in this work. In addition, due to the poor DFT description for the high-spin ground state of O_2, $G_{O2,g}+4G_{H2,g}-2G_{H2O,l}=4.92$ eV is used to compute the G of the gas-phase O_2 ($G_{O2,g}$). The ΔG for the above four OER steps could be described as $\Delta G_1 = \Delta G_{HO*}$, $\Delta G_2 = \Delta G_{O*} - \Delta G_{HO*}$, $\Delta G_3 = \Delta G_{HOO*} - \Delta G_{O*}$, and $\Delta G_4 = 4.92 - \Delta G_{HOO*}$. The overpotential η of OER (η^{OER}) was calculated by equation (9) [4]:

$$\eta^{OER} = \frac{\max\{\Delta G_a, \Delta G_b, \Delta G_c, \Delta G_d\}}{e} - 1.23 \quad (9)$$

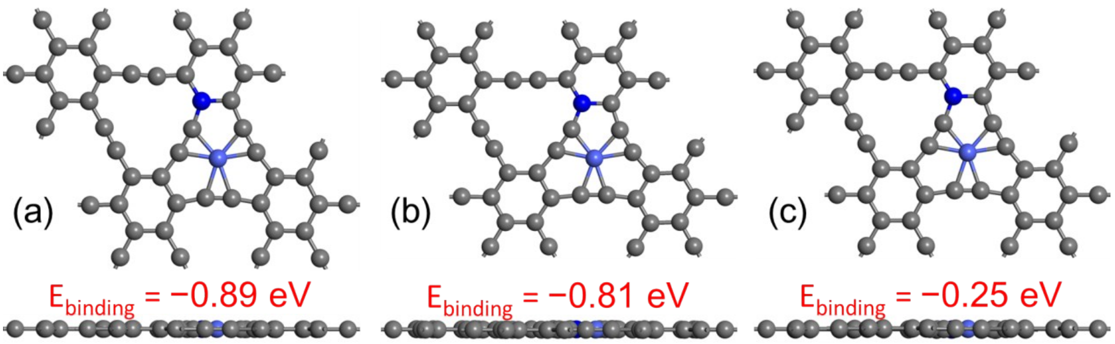

Fig. S1 Optimized structures of Co@N$_1$-GY under tensile strain: (a) *a*-uniaxial of 6%, (b) *b*-uniaxial of 6%, and (c) biaxial of 4%.

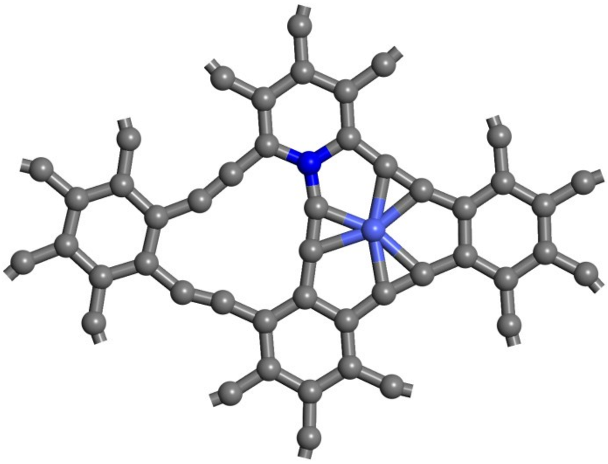

Fig. S2 Optimized structures of Co@N$_1$-GY under biaxial tensile strain of 4%.

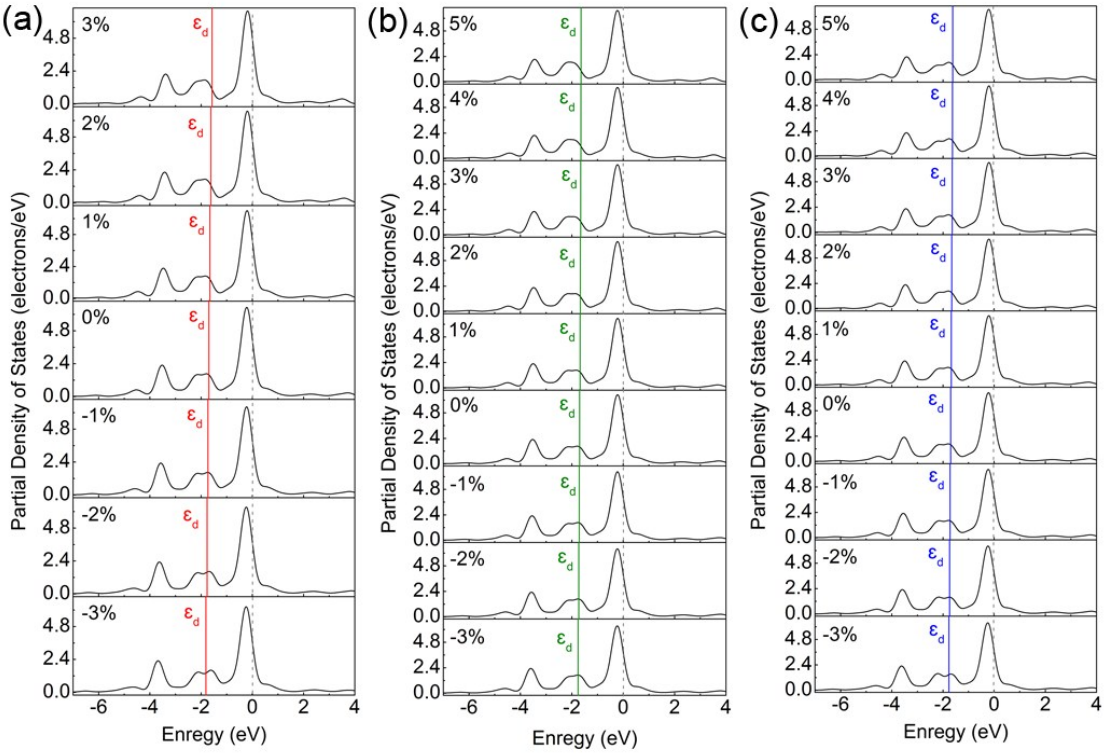

Fig. S3 Calculated partial density of states of the Co atoms in Co@N$_1$-GY with (a) biaxial strain from -3% to 3%, (b) *a*-, and (c) *b*-uniaxial strain from -3% to 5%. The *d* band center of Co atom is marked by the red, green, and blue lines, respectively. The Fermi level is set as zero, as shown in the gray dashed line.

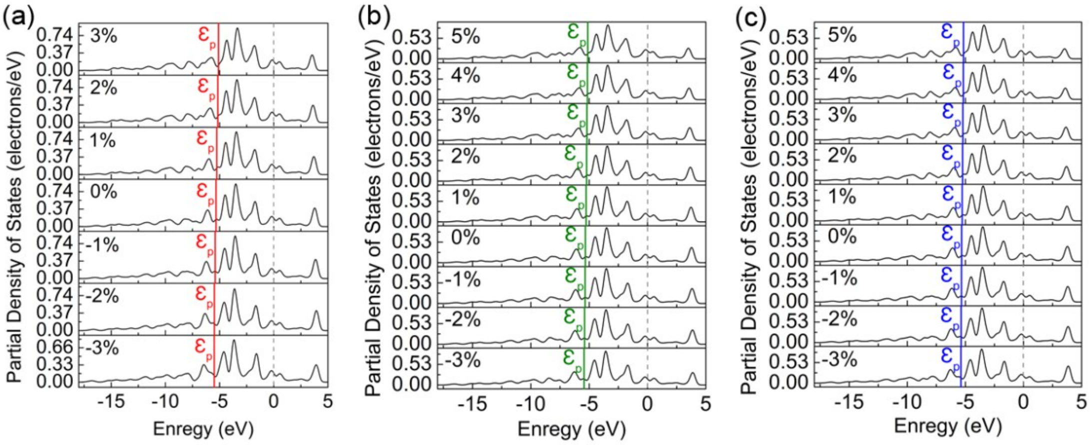

Fig. S4 Calculated partial density of states of the C atoms in Co@N$_1$-GY with (a) biaxial strain from -3% to 3%, (b) *a*-, and (c) *b*-uniaxial strain from -3% to 5%. The *p* band center of C atom is marked by the red, green, and blue lines, respectively. The Fermi level is set as zero, as shown in the gray dashed line.

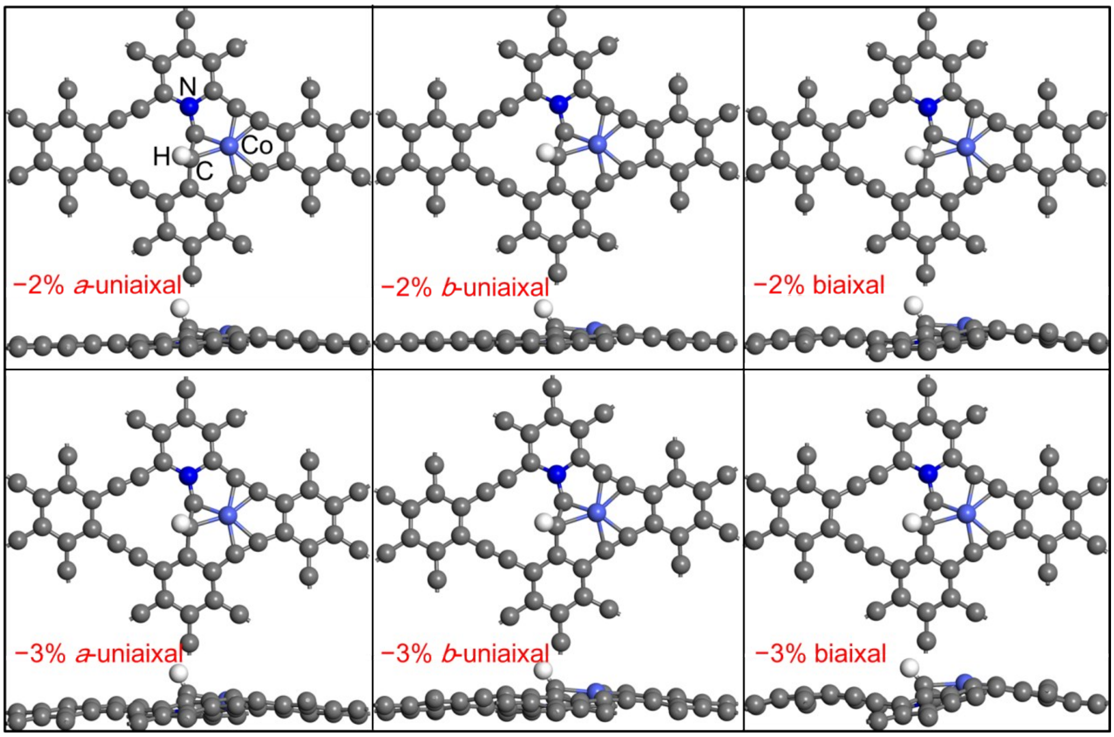

Fig. S5 Top and side views of optimized stable H-Co@N_1-GY configurations under −2% and −3% compressive lattice strain.

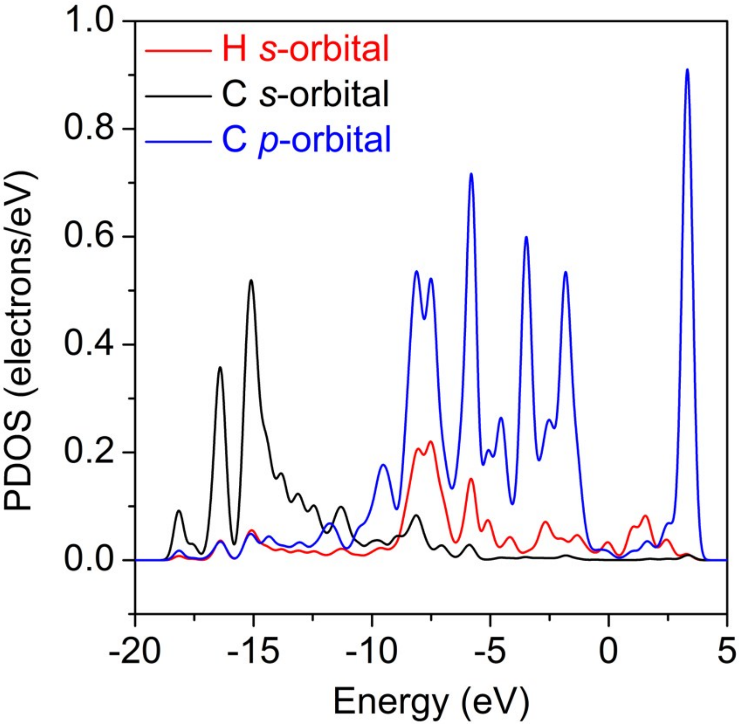

Fig. S6 Partial density of states of the unstrained H-Co@N_1-GY configuration (H is adsorbed on the C atom site connected with the Co atom).

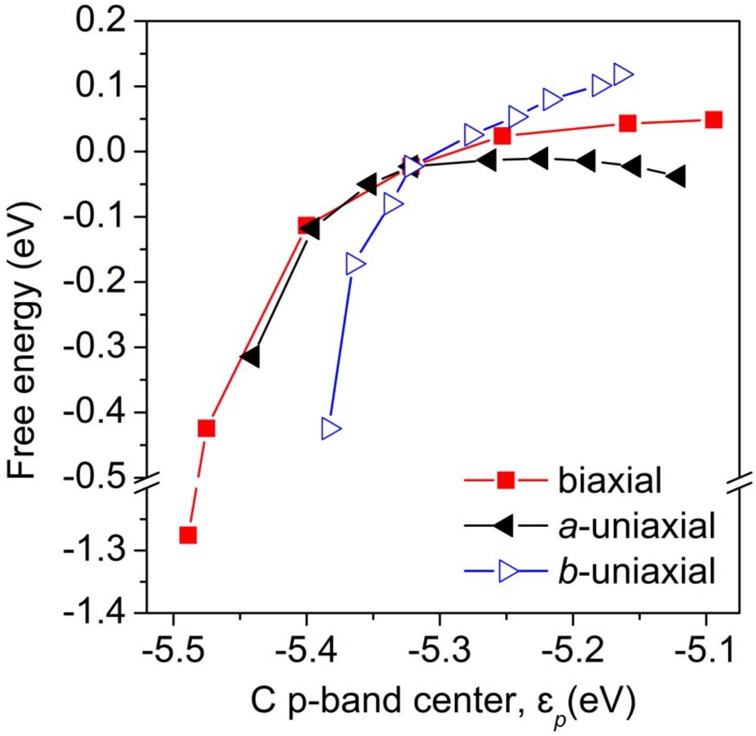

Fig. S7 Calculated free energy diagram for hydrogen evolution of Co@N_1-GY catalyst versus *p*-band center of C atom at standard conditions (pH=0, U=0 relative to the standard hydrogen electrode, and 298.15 K).

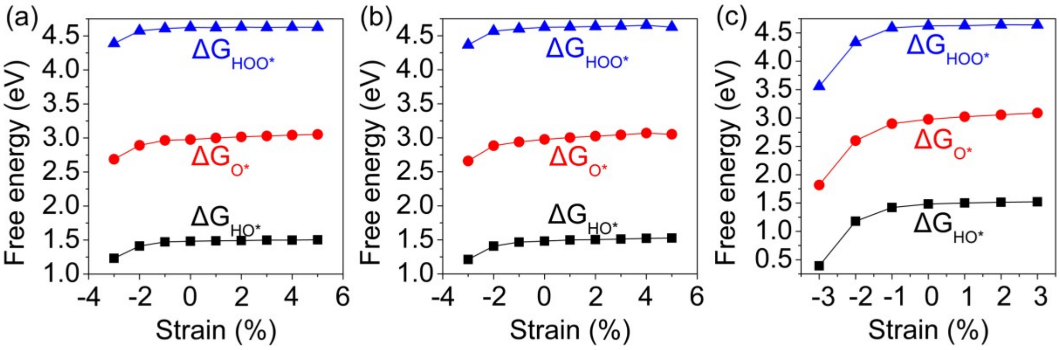

Fig. S8 The change in adsorption free energies of the oxygen intermediates in OER versus different lattice strain-optimized Co@N_1-GY catalyst: (a) *a*-uniaxial lattice strain, (b) *b*-uniaxial lattice strain, and (c) biaxial lattice strain.

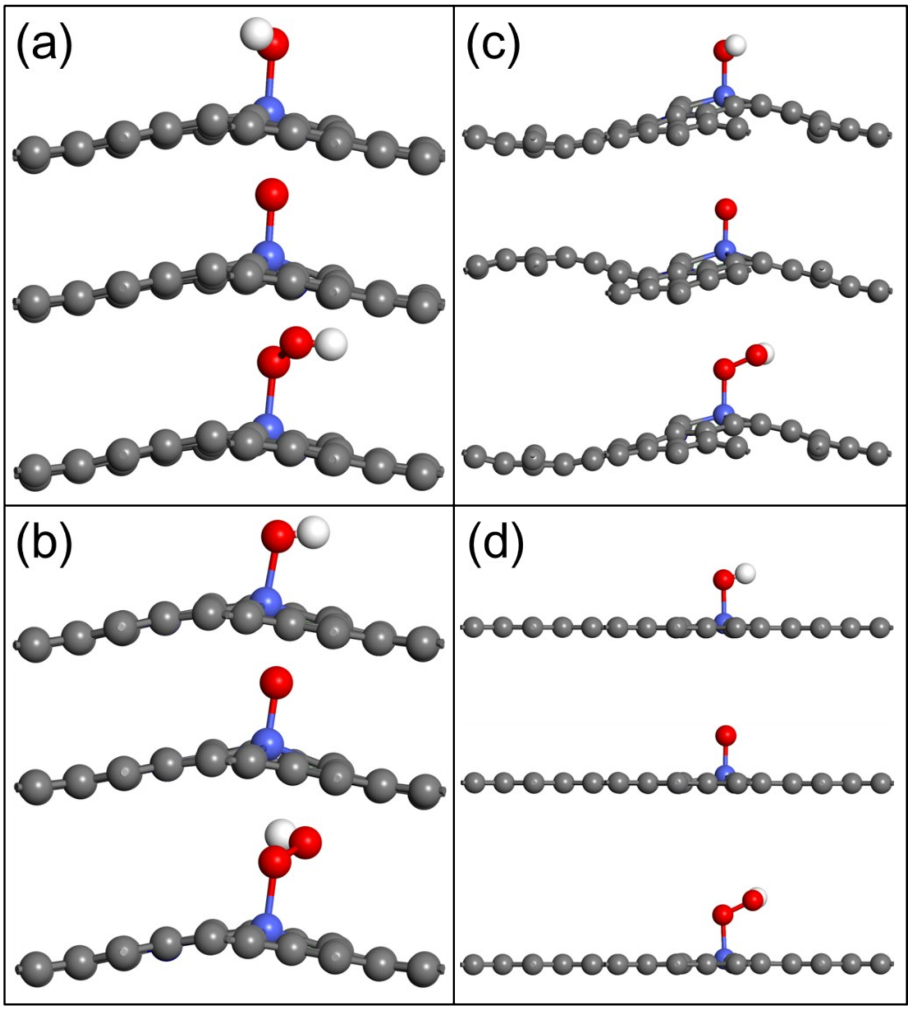

Fig. S9 Optimized stable adsorption configurations of oxygen intermediates (HO*, O*, and HOO*) on strained Co@N_1-GY catalyst: (a) -3% *a*-uniaxial compressive strain, (b) -3% *b*-uniaxial compressive strain, (c) -3% biaxial compressive strain, and (d) +3% biaxial tensile strain. The grey, blue, red, and white balls represent the carbon, cobalt, oxygen, and hydrogen atoms, respectively.

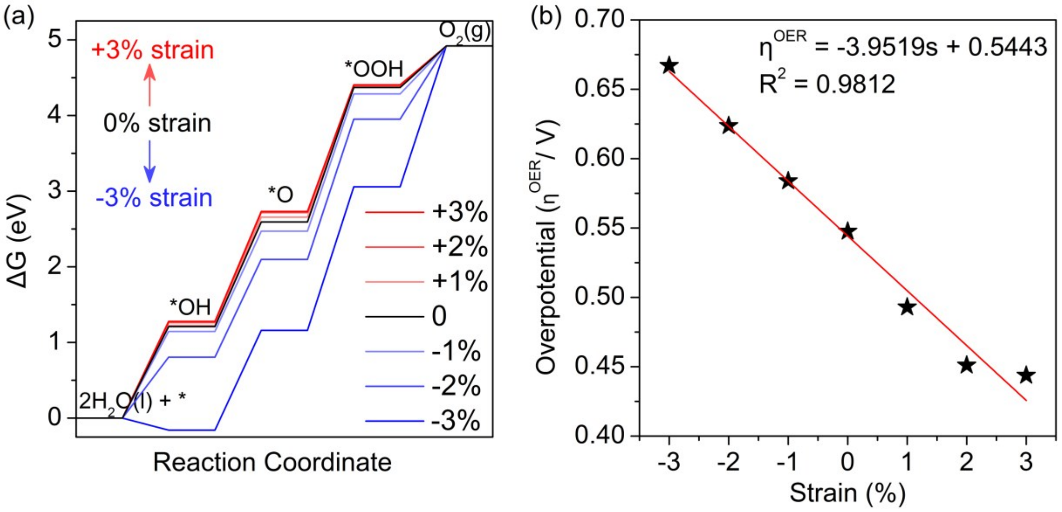

Fig. S10 (a) Calculated free energy diagram for the OER over the Co site of Co@GY catalyst with biaxial strain changing from -3% to 3% at U=0 V, (b) overpotential of OER for the Co@GY catalyst as a function of biaxial strain.

Table S1 Vibrational frequencies of the intermediates adsorbed on Co@GY catalysts.

System	Vibration Frequencies (cm $^{-1}$)
H*- Co@GY	390.66, 392.07, 2129.41
HO*- Co@GY	171.71, 185.91, 202.28, 549.43, 944.16, 3639.02
O*- Co@GY	190.5, 191.79, 735.99
HOO*- Co@GY	104.51, 142.18, 173.45, 276.49, 353.87, 520.01, 832.4, 1325.4, 3570.09

Table S2 The zero-point energy (ZPE) and entropic corrections (TS) in determining the free energy of reactants, intermediates, and products adsorbed on catalysts at 298K. For the adsorbates, the ZPE value is not sensitive to the metal and coordination since they have close value.

Species	ZPE(eV)	TS(eV)
H_2O	0.56	0.67
H_2	0.27	0.41
H*	0.16	0
O*	0.05	0
HO*	0.36	0
HOO*	0.40	0

[1] J.K. Nørskov, T. Bligaard, A. Logadottir, J.R. Kitchin, J.G. Chen, S. Pandelov, U. Stimming, Trends in the Exchange Current for Hydrogen Evolution, J. Electrochem. Soc., 152 (2005) J23-J26.

[2] J.K. Nørskov, J. Rossmeisl, A. Logadottir, L. Lindqvist, J.R. Kitchin, T. Bligaard, H. Jónsson, Origin of the Overpotential for Oxygen Reduction at a Fuel-Cell Cathode, The Journal of Physical Chemistry B, 108 (2004) 17886-17892.

[3] Q. Tang, D.-e. Jiang, Mechanism of Hydrogen Evolution Reaction on 1T-MoS2 from First Principles, ACS Catalysis, 6 (2016) 4953-4961.

[4] I.C. Man, H.-Y. Su, F. Calle-Vallejo, H.A. Hansen, J.I. Martínez, N.G. Inoglu, J. Kitchin, T.F. Jaramillo, J.K. Nørskov, J. Rossmeisl, Universality in Oxygen Evolution Electrocatalysis on Oxide Surfaces, ChemCatChem, 3 (2011) 1159-1165.